Hydrodynamic aspects of aerosols pool scrubbing

Mohamad Farhat, Philippe Nerisson, Laurent Cantrel, Maxime Chinaud, Olivier Vauquelin

Hydrodynamic aspects of aerosols pool scrubbing

M. FARHAT[*1,2], P. NERISSON[1], L. CANTREL[1], M. CHINAUD[2], O. VAUQUELIN[2]

[1]Institut de Radioprotection et de Sûreté Nucléaire (IRSN), 13115 St Paul Lez Durance
[2]Aix-Marseille Université, IUSTI UMR 7343, 5 rue Enrico Fermi, 13453 Marseille

Abstract

Pool scrubbing has shown potential efficiency to reduce the release of fission products, especially in aerosol forms, into the environment. Considering the large test conditions where pool scrubbing might be encountered, there is still a lack of systematic analysis of this phenomenon, especially its dependence on different hydrodynamic regimes. Experimental work was carried out, where hydrodynamic and decontamination factor measurements were performed. Caesium iodide aerosols were injected into the TYFON facility for different flow regimes ($0.08 \leq We \leq 15\ 600$) by varying both injection flowrate Q_{inj} and nozzle size D_0, in which their effects were examined. The Weber number (We) has shown to be capable of characterizing the decontamination factor, when comparing this work with data from literature. Moreover, the different flow regimes induced different sensitivities of aerosol removal mechanisms, where a minimum scrubbing is observed in the transition between bubbly and jet regime. The effect of pool submergence was also investigated in case of bubbly and jet regimes, in which the contribution of residence time and inertial impaction to pool scrubbing was shown.

Keywords: Pool scrubbing; Hydrodynamics; Decontamination factor; Aerosol

Nomenclature

d_p	Mass median aerodynamic diameter	[m]
D_0	Nozzle diameter	[m]
D_{col}	Column diameter	[m]
DF	Decontamination factor	[-]
DF_{imp}	Decontamination factor by inertial impaction	[-]
Eff	Efficiency by inertial impaction	[-]
F_d	Dilution factor	[-]
f_G	Frequency of globule formation	[Hz]
H_{pool}	Submergence of the pool	[m]
$\dot{m}_{in}$	Inlet aerosol mass flowrate	[kg.s^{-1}]
$\dot{m}_{out}$	Outlet aerosol mass flowrate	[kg.s^{-1}]
Q_{inj}	Injected air volume flowrate	[m^3.s^{-1}]
$Q_{sampling}$	Sampling flowrate	
St	Stokes number: $St = \frac{\rho_p \ {d_p}^2 \ U_{inj}}{18 \ \mu_g \ D_0}$	[-]
$\tau_{characteristic}$	Characteristic time of the pool	[s]
$\tau_{residence}$	Average residence time in the pool	[s]
U_{inj}	Gas injection velocity: $U_{inj} = \frac{Q_{inj}}{\pi \ D_0^2/4}$	[m.s^{-1}]
U_{sup}	Superficial velocity: $U_{sup} = \frac{Q_{inj}}{\pi \ D_{col}^2/4}$	[m.s^{-1}]
V_G	Globule volume	[m^3]
V_{TYFON}	Volume of TYFON facility	[m^3]
We	Nozzle Weber number: $We = \frac{\rho_g \ {U_{inj}}^2 \ D_0}{\sigma}$	[-]
Y	Altitude above the nozzle	[m]

Greek symbols

ρ_g	Gas density	[kg.m^{-3}]
ρ_l	Liquid density	[kg.m^{-3}]
ρ_p	Particle density	[kg.m^{-3}]
σ	Surface tension	[N.m^{-1}]
σ_g	Geometric standard deviation	[-]
μ_g	Air dynamic viscosity	[Pa.s]

1. Introduction

The featuring of nuclear power plants with accident management systems aims mainly at mitigation and reducing the release of fission products into the environment [1]. Mitigation, hence, refers for all processes that may lead to the trapping and retention of containment atmosphere, thus, reducing the potential risks of radioactive material release into the environment. Efficient engineering systems for fission products removal are containment sprays, suppression pools in boiling water reactors, and filtered containment venting systems FCVS in pressurized water reactor. The efficiency of these systems is expressed in terms of Decontamination Factor DF, which is defined as the ratio of the quantity of fission products at the inlet to the outlet of the filtration system.

$$DF = \frac{\dot{m}_{in}}{\dot{m}_{out}} \tag{1}$$

The concept of pool scrubbing as filtration mechanism was widely spread after the accident of the Three Mile Island TMI-2 [2, 3], where many NPPs aimed at installing FCVSs to mitigate the radiological consequences of core meltdown accidents. The Chernobyl accident (26 April 1986) brought additional attention to the issue of source term mitigation [2-5]. Moreover, in BWR meltdown accidents like in Fukushima accident (March 11th, 2011), suppression pools are involved as passive systems for fission product trapping, where pool scrubbing has shown main importance to the evaluation of fission products releases [6]. The importance of pool scrubbing relies on its efficiency in reducing the release of fission products (especially in form of aerosols) such as iodine compounds, of which their volatility and radiotoxicity are a public concern. Wet FCVS, where pool scrubbing is mainly considered, are mostly efficient in aerosol scrubbing than gaseous iodine. AREVA designed the standard FCVS on the basis to have a DF > 100 000 for large aerosols, DF > 10 000 for small aerosols, DF > 200 for molecular iodine, and DF > 5 for organic iodine [7].

Hence, pool scrubbing was extensively investigated in the 1980s and 1990s in several large research programs [8-15]. In this period, research institutes and organizations realized experimental programs and developed, upon the established experimental databases, pool scrubbing codes such as SPARC, BUSCA, and SUPRA. Although that most of developed codes haven't shown good predictions [16], the pool scrubbing mechanism showed a high efficiency of trapping fission products especially for aerosols (DF > 10). Post the accident of Fukushima, many follow-up actions were taken notably considering the implementing and enhancing of FCVSs [1, 5, 17-20]. Therefore, research programs on improving safety measures resumed and programs within the international framework were launched, in order to better characterize the mechanism of pool scrubbing [21-30].

It is observed that the investigation of pool scrubbing's dependence on control parameters is not simple issue, as comparison between experimental outcomes should be done carefully. For example, the impact of injection flowrate has shown opposite senses regarding the retention mechanisms between a facility and another, which is due to the scope of test conditions and facility scale parameters. An increase in decontamination factor was reported with the increase of injection flowrate in Herranz et al. [22], Jung et al. [23], and Yoon et al. [24]. However, a decrease of DF was reported as injection flowrate increased in Xu et al. [25]. Moreover, other parameters have shown different sensitivities/trends to retention mechanism, even if they showed a unique sense (favoring or hindering) in most experimental programs (pool submergence, steam mass fraction). For example, DF was reported to increase with

submergence in different trends (linearly or exponentially) in Xu et al. [25], Li et al. [27], Li et al. [28], and Dehbi et al. [31]. Obviously, this reveals how trapping of aerosols is dependent on a set of experimental parameters. Consequently, attempts of describing the experimental aspects of pool scrubbing is essential, as it relies on set of physical and chemical mechanisms leading to the trapping of fission products.

While in form of aerosols, these processes are referred by aerosol removal mechanisms. The latter mechanisms are the sum of Brownian diffusion, thermophoresis, inertial and centrifugal impaction, condensation, and sedimentation [16]. Among these mechanisms, each one has its own significant impact considering the hydrodynamics of the gas flow in the pool. Therefore, the hydrodynamics of bubble are highly regarded in the scrubbing efficiency.

Ramsdale et al. [8] divided the flow in pool scrubbing facilities into three hydrodynamic zones: the injection zone, transition zone, and bubbles rise zone (bubbles swarm). Bubbles velocities in the different zones are regarded in the determining of bubbles residence time, such as the bubbles rising velocity in the injection zone and the terminal velocity in the bubble rise zone. With the increase of residence time, the aerosol removal mechanisms act for a greater period of time in the pool, thus increasing the efficiency of pool scrubbing [26, 32, 33].

In the injection zone, which is the zone near the nozzle, different flow morphologies can prevail. However, two main types of regimes are widely considered: the bubbly regime and jet regime. The bubbly regime is characterized by the formation of gas bubbles at the top of nozzle, which shapes, or sizes can vary according to the flow conditions. This regime also comprises the aperiodic formation and successive coalescence of the bubbles, where Farhat et al. [34] have characterized the globule formation following these coalescences. They reported that classical approaches are not consistent in characterizing the hydrodynamics in the aperiodic formation, and then they provided a phenomenological approach, which is shown to be more consistent. Whereas, when the gas momentum increases so that the surface tension of air/liquid collapses, a critical shift in the flow morphology prevails introducing the jetting regime.

Owing to the different hydrodynamic aspects of each flow regime, it is necessary to distinguish and classify the flow regimes, throughout the different experimental programs, using dimensionless numbers. The use of dimensionless numbers reduces the number of parameters describing test matrix, which is relevant and necessary in the case of pool scrubbing experiments taking in consideration the large number of experimental parameters comprised in pool scrubbing experimental campaigns. This enables the characterizing of different physical phenomena such as inertial processes, consequently, providing a comparison between experimental works of different scales.

Since the inertial gas momentum is the dominant parameter in the flows relevant to pool scrubbing, Weber number is considered the key parameter for the description of flow regimes. It has been already used for this purpose, notably for the transition from bubbly to jet regime [35, 36]. This dimensionless number compares the inertial forces or gas momentum to the surface tension such that:

$$We = \frac{\rho_g \, U_{inj}{}^2 \, D_0}{\sigma} \tag{2}$$

where ρ_g is the gas density, U_{inj} is the injection velocity, D_0 is the nozzle diameter, and σ is the surface tension. Zhao et al. [36] applied combined Kelvin–Helmholtz and Rayleigh–Taylor

instability analysis in order to obtain the critical Weber number for transition from bubbling to jetting regime. The critical Weber number was given by We = 10.5 $(\rho_l / \rho_g)^{0.5}$, such that $We_{critical}$ = 306 at ambient temperature (25 °C). Despite the criterion of Zhao et al. [36], other criterions were provided based on Reynolds number such in [37, 38], where different critical values have been reported. For that, and to avoid overlapping of regimes, a transition regime is generally considered between the bubbly and jetting regime.

The present paper reports the hydrodynamic aspects affecting the processes of aerosol trapping through different flow regimes. Owing to this objective, we conducted experiments coupling the hydrodynamic measurements of carrier gas injected into liquid pool as well as the trapping of aerosols suspended in a carrier gas. Regarding the hydrodynamics, the possible influence of carrier gas contamination on bubbling is investigated, by characterizing the hydrodynamics in the injection zone. For that, globules volumes and frequencies were determined for different flow conditions. On the other hand, and while characterizing the globule dynamics, decontamination factor measurements were carried out to quantify the trapping of aerosols. Based on severe accident measurements used to assess the chemical forms of iodine in containment, caesium iodide (CsI) is usually considered to be one the dominant aerosol form to be released [1, 2] in terms of radiological consequences. Moreover, it was the most common aerosol used in the experimental programs for its relevance in nuclear accidents and associated post releases [16]. For that, caesium iodide was generated to be carried in form of aerosol particles. Thereafter, experiments were conducted to study the trapping's dependence on the different flow regimes. In this study, we investigated the impact of injection flowrate Q_{inj}, nozzle size D_0, and submergence H_{pool}, to better characterize the dependence of the decontamination factor on these parameters.

2. Materials and methods

Experiments were carried out on the TYFON facility (Trapping and hYdrodynamics of FissiON products behaviour in pool scrubbing), which allows coupling the measurements of bubble dynamics and decontamination factor. For the quantification of caesium iodide quantities upstream and downstream the water bath, samples were taken to be analysed by Inductively Coupled Plasma Mass Spectrometry (ICPMS) to determine the decontamination factor. The facility permits modifying the test parameters such as gas flowrate, its temperature, size of injector nozzle (oriented vertically), its submergence in the pool, and the temperature of the pool. Eventually, this allows to investigate the dependence of the bubble hydrodynamics and decontamination factor on the different experimental aspects.

2.1 Experimental setup

Figure 1 shows the TYFON facility where experiments on pool scrubbing for caesium iodide aerosols were conducted. The pool column is of 500 mm internal diameter (D_{col}) and afford pool submergence of 1.3 m, which corresponds to a volume of 250 L. The interior walls of the column are made up of stainless steel ''mirror polished'' to effectively prevent the adsorption of iodine on its surfaces. To adjust the pool temperature and submergence, thermocouples and pressure sensors are distributed between the injection and the height of the free surface of the pool.

Figure 1- TYFON facility

2.2 Hydrodynamic measurements in the injection zone

Two glass windows are aligned at two different altitudes above the nozzle position (Y = 5 cm, Y = 75 cm) permitting image acquisitions using high-speed camera, ''Phantom Speed sense" VEO-E'', which could take 3000 images per second at resolution 1280 × 800 pixels. The injection system permits the modification of the nozzle tray, where four sizes of nozzle were mounted (D_0 = 2 mm, D_0 = 5 mm, D_0 = 10 mm, and D_0 = 20 mm) as shown in Figure 2.

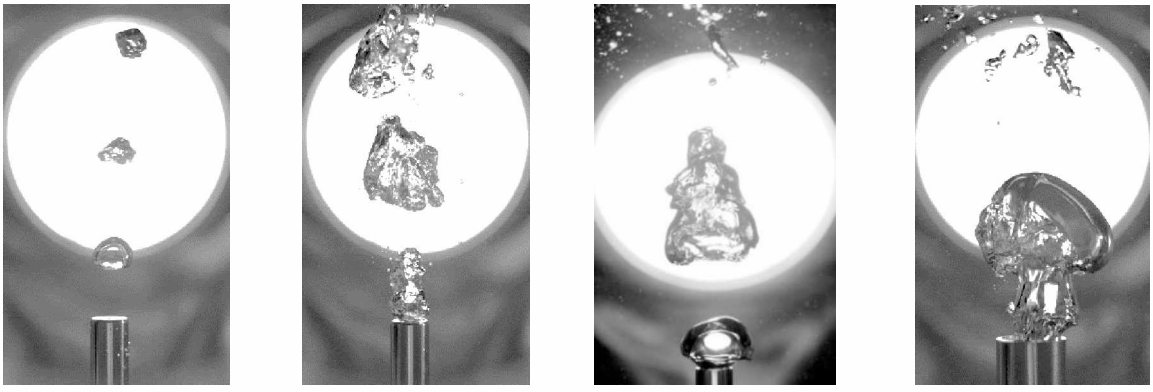

(a) (b) (c) (d)

Figure 2- The nozzle injectors where gas was injected to the column. (a) D_0 = 2 mm, (b): D_0 = 5 mm, (c) D_0 = 10 mm, (d) D_0 = 20 mm.

The variation of nozzle size, within the range of flowrates (0 – 17 m^3/h), permits to cover wide range of Weber number ($0.07 < We < 20\,000$), in other words, to induce wide range of flow regimes. Through image treatment and tracking of bubbles formation above the nozzle, bubble dynamics were characterized as detailed in Farhat et al [34]. Measurements were performed for air flow injection, with and without caesium iodide, in order to investigate the influence and the impact of contamination on the dynamics of the carrier gas. More specifically, this investigation took place in the injection zone.

2.3 Decontamination factor measurements

Depending on the different form of the iodine compound, the systems of their generation or injecting into the TYFON facility varies, as well as the sampling process, and the analysis technique for their measurements. The duration of tests varied from 2 to 5 hours, according to the characteristic time $\tau_{characteristic}$ for the carrier gas to occupy the facility volume (250 L). This is the time required for one renewal of the volume of TYFON by the injected gas:

$$\tau_{characteristic} = {V_{TYFON}}/{\dot{Q}_{injection}} \quad (3)$$

Thus, to reach a steady state, duration of test t is fixed at least such as $t \geq 5\ \tau_{characteristic}$.

2.3.1. Configuration of CsI tests

Caesium iodide aerosols are generated using Palas AGK 2000 generator shown in Figure 3. The compressed air injected into the AGK, containing the aqueous solution of caesium iodide, nebulizes the solution so that dehydrated aerosols are fed into the gas flow at the downstream of the AGK. The median mass aerodynamic diameter (MMAD) for CsI aerosols is 0.8 µm (with a dispersion $\sigma_g \approx 2$), and the average aerosols mass flowrate is 10 mg/h. This aerosol generation has been implemented previously in studies dealing with fission products transfer in nuclear severe accident conditions [39]. Aerosol distribution parameters (MMAD, σ_g) have been previously determined with DEKATI impactor. Characterization campaigns have shown reproducible results for this granulometry on a high number of tests. The regulation of injection flowrate into TYFON is subjected to a range of flowrates, due to the aerosol generator's operational pressure. For that, another injection line (compressed air) is considered.

The amount of CsI aerosols injected into TYFON corresponds to the amount of CsI trapped in the pool added to the amount of CsI that released out the column through the duct. Therefore, DF is calculated such that:

$$DF = \frac{m_{in_{(t)}}}{m_{out_{(t)}}} = \frac{m_{trapped_{(t)}} + m_{out_{(t)}}}{m_{out_{(t)}}} \quad (4)$$

For the quantity of CsI aerosols trapped in the column, a valve permits to collect liquid sample from the pool inside the column. At the end of test, agitation of the column for around half an hour was induced by injecting clean gas at high flowrates. This aims to obtain a good mixing. After that, and while emptying the column from its bottom, samples were also taken in order to compare with the concentrations taken from the middle valve. The analysis of concentrations

showed similar concentrations in samples from the bottom and from the middle of the column. Thus, the samples can be considered as representative of the column concentration.
For the quantity of CsI released out the column in the downstream, the gas is vented from the main exhaust through the cane at a flowrate in order to maintain the same velocity of carrier gas in the exhaust and the sampling line. This isokinetic sampling method [40] aims at better representing the actual outflow in the exhaust in terms of aerosol concentration. To compensate, a dilution factor F_d (ratio of injection flowrate to sampling flowrate) permits to represent the actual CsI amount in the downstream as shown in eq.(5).

$$F_d = \frac{Q_{inj}}{Q_{sampling}} \tag{5}$$

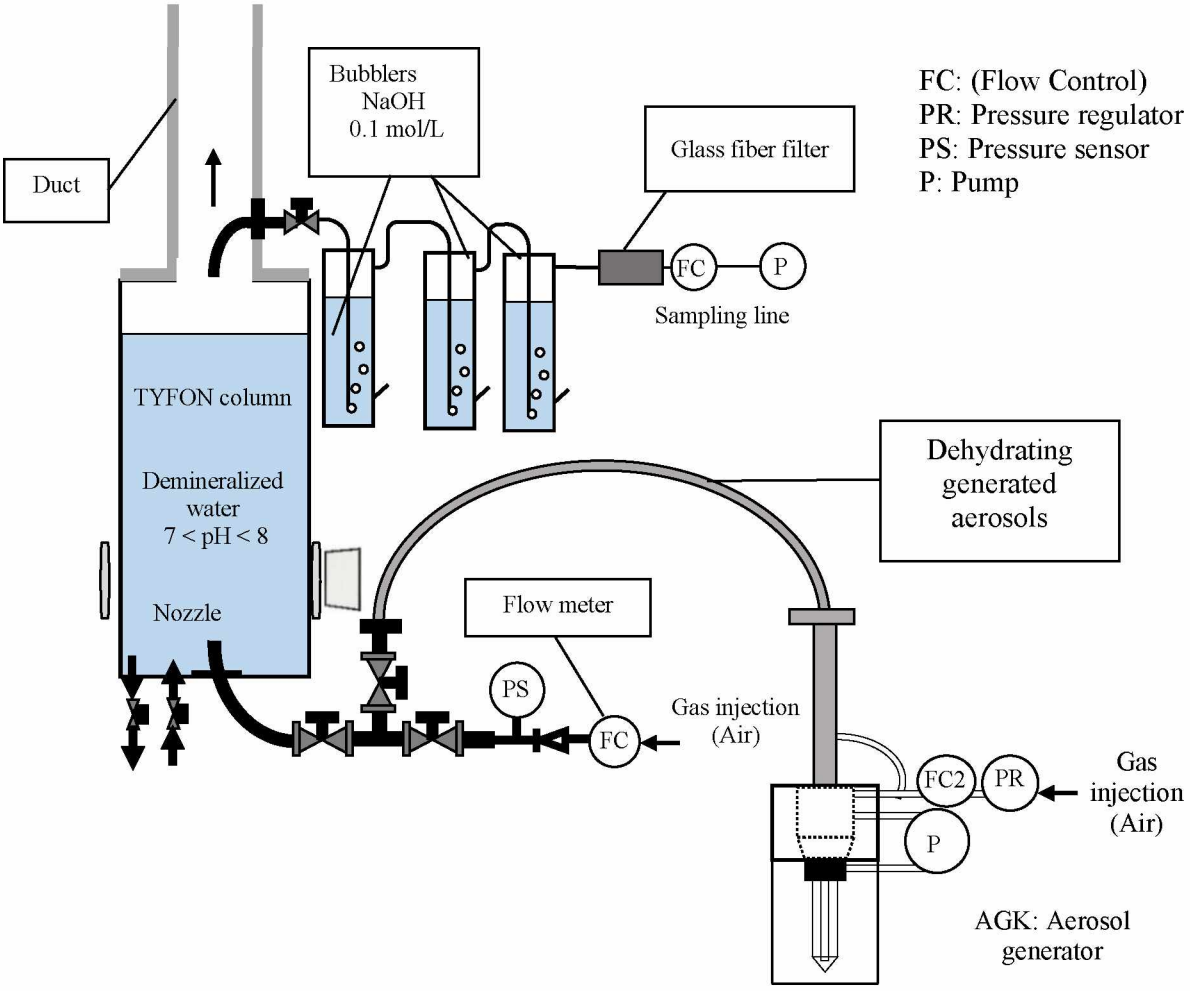

Figure 3- Caesium iodide configuration on TYFON facility

The sampling system is composed of 3 bubblers, glass fiber filter, flowmeter, and a pump as shown in Figure 3. The three bubblers of known masses are filled with 0.1 molar sodium hydroxide to have same submergence, and then weighed. The glass fiber filter, whose filter integrity permits to trap all the outgoing aerosols from the bubblers, is the end of the sampling line.

Taking in consideration the aerosol deposition on the surfaces, notably in the sampling system (isokinetic cane, pipes), washing was performed at the end of the experiment in order to collect all the deposited quantity of CsI aerosols.

2.3.2. Test matrix

Table 1 presents the test matrix on the retention of CsI aerosols. The main investigation was to study the dependence of scrubbing on the different test conditions, which influenced the flow regimes represented by the Weber number. For this study, we conducted the experiments with mainly varying the injection flowrate Q_{inj} and the size of the nozzle D_0. Other tests were performed to investigate the impact of pool submergence H_{pool}, especially for the bubbling regime where the residence time of bubbles is much important than in jetting regime.

Table 1- Integral test matrix of pool scrubbing tests

Test	H_{pool} (cm)	D_0 (mm)	Q_{inj} (L/min)	U_{inj} (m/s)	U_{sup} (cm/s)	Weber
1	100	2	131.0	690	1.112	15600
2	100	2	74.2	391	0.630	5000
3	100	2	33.2	175	0.282	1000
4	100	2	8.4	44.2	0.071	64
5	100	5	131.2	111	1.114	1000
6	100	5	77.6	65.4	0.659	350
7	100	5	59.4	50.0	0.504	205
8	100	5	33.3	27.9	0.283	64
9	100	5	23.5	19.8	0.199	32
10	100	5	9.2	7.8	0.078	4.93
11	100	20	73.7	3.9	0.626	4.93
12	100	20	9.2	0.5	0.078	0.08
13	30	20	9.2	0.5	0.078	0.08
14	10	20	9.2	0.5	0.078	0.08

The other conditions were the same for all the experiments to exclude their influence. Compressed air was used as the carrier gas at ambient temperature, so no steam fraction was considered. The temperature of carrier gas and pool were adjusted such that $T_{pool} = T_{gas} = 25$ °C, and pH of the pool was set around 7. Samples from the column were measured and verified by a pH meter, then the pH was adjusted by adding few milliliters of 1 molar sodium hydroxide NaOH to the demineralized water ($7 < pH < 8$) in the column. The size of aerosols depends strongly on the concentration of solution provided to the aerosol generator. The solutions were all prepared to have a concentration of 10 g/l to get aerodynamic mass median diameter of particles around 0.8 µm. In Table 2, the controlled variables for all the tests are shown.

Table 2- Controlled variables of the test matrix

Carrier Gas	Gas temperature (°C)	Pool temperature (°C)	Pool pH	Aerosol/size (µm)	Mean mass flowrate (mg/h)
Air	25	25	~7	CsI / 0.8	10

3. Results and discussion

3.1 Impact of carrier gas composition in the injection zone

In the injection zone in bubbly regime, globules are formed, after the coalescence of departed bubbles. In order to reveal impact of contamination of carrier gas on the globule dynamics, the globules formations in injection zone were examined and compared with non-contaminated air. The globule volume is computed numerically by considering a unitary volume corresponding to a pixel in a binarized image, as presented in our detailed technique in Farhat et al. [34].

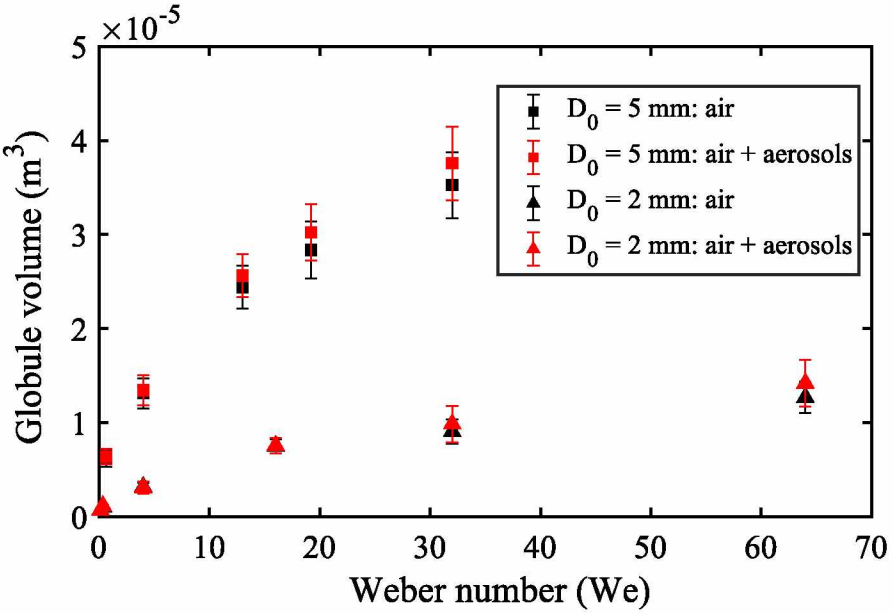

Figure 4- Potential impact of caesium iodide aerosols on globule volumes for different hydrodynamic regimes.

Figure 4 reports no significant influence of this contamination on the globule sizes, for the different sizes of nozzles and at different injection flowrates. In fact, this was expected because caesium iodide aerosols are considered soluble in water, moreover the size's ratio of the aerosol's particles to average globule volumes is less than 5×10^{-3}. Knowing it, the inlet concentration of injected CsI solution and depending on mass concentration, this ratio seems to be low and aerosol presence can be considered to have no influence on hydrodynamics phenomena of bubble-air flow [40]. Moreover, considering the domination of the inertial forces

leading to large globule volumes, it is suggested that the carrier gas composition is not affecting its surface tension properties, thus, its volume.

Globule formations are affected by the wake and entrainment of the flow, depending on the injection flowrate. Thus, in order to study the possible effects of contamination on the globule formation, the characterization of the frequency of bubbling should be considered. Globule frequency is determined by tracking the coalescences of bubbles leading to the formation of a large bubble [34]. In addition to negligible effect of contamination on globule volumes, the different test configurations have shown no effect of aerosols also on the globule frequency as shown in Figure 5. In fact, the average frequency of globules at different flowrates tends to be stable at constant frequency. Davidson et al. [40] suggested that a maximum frequency of air bubbles formation is reached beyond a certain flowrate for certain nozzle size. Moreover, Clift et al. [41] stated that frequency becomes weakly dependent on flowrate in dynamic regimes. In our experiments, as We > 1, the further increase in injection flowrate, consequently Weber number, affect only the volume of globules, whereas the frequency is similar for the different sizes of nozzles.

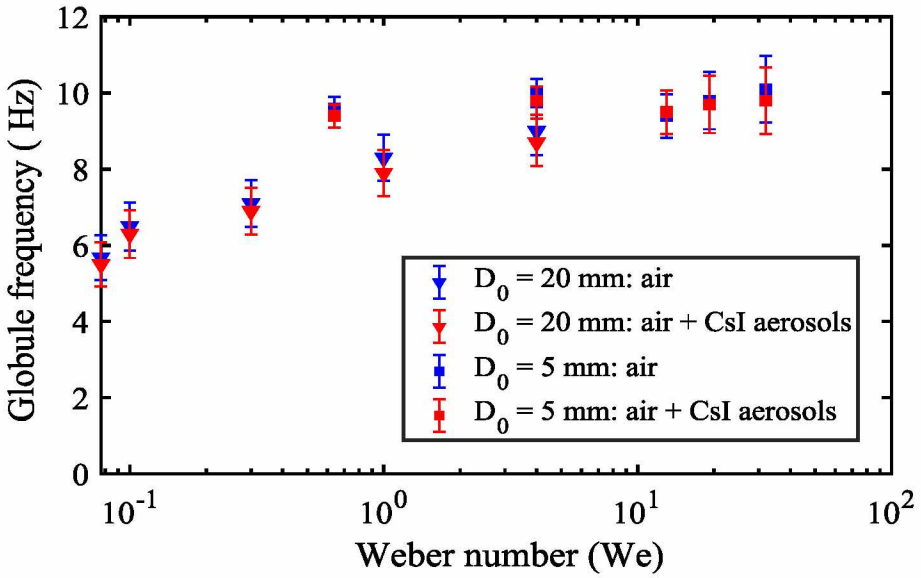

Figure 5- Impact of caesium iodide aerosols on globules frequency.

As no impact of contamination on globule volume and frequency is observed, it can be deduced that globule formation is also not affected. This suggests that, as injection flowrate increases, the influence of inertial forces will increase and so is their dominance over the possible effects of gas contamination.

3.2 Aspects of CsI aerosols' scrubbing

Table 3 shows the experimental measurements of the decontamination factors.

Table 3- Summary of the experimental decontamination factors of

Test	Weber	Flow regime	DF (± 10%)
1	15600	Jet	285
2	5000	Jet	63
3	1000	Jet	22
4	64	Bubbling	8
5	1000	Jet	26
6	350	Transition	14
7	205	Transition	5
8	64	Bubbling	5
9	32	Bubbling	7
10	4.93	Bubbling	31
11	4.93	Bubbling	31
12	0.08	Bubbling	46

The pool scrubbing experiments shown in Table 3 examined different hydrodynamic flow regimes by varying the nozzle size D_0 and injection flowrate Q_{inj}, while maintaining the pool submergence such that H_{pool} = 100 cm.

3.2.1. Form of trapped caesium iodide

CsI aerosols were trapped in the pool and the bubblers, and also deposited on the tubing connecting the sampling line, as well as depositions on the fiber filter at the end of the sampling line. Sampling from the pool and the bubblers were performed each 30 minutes, where the duration of injection of iodine compound for each test varied between 2 and 4 hours (see 2.3.) An example of evolutions of retention in the pool and sampling line (bubblers) as a function of time is shown in Figure 6 and Figure 7.

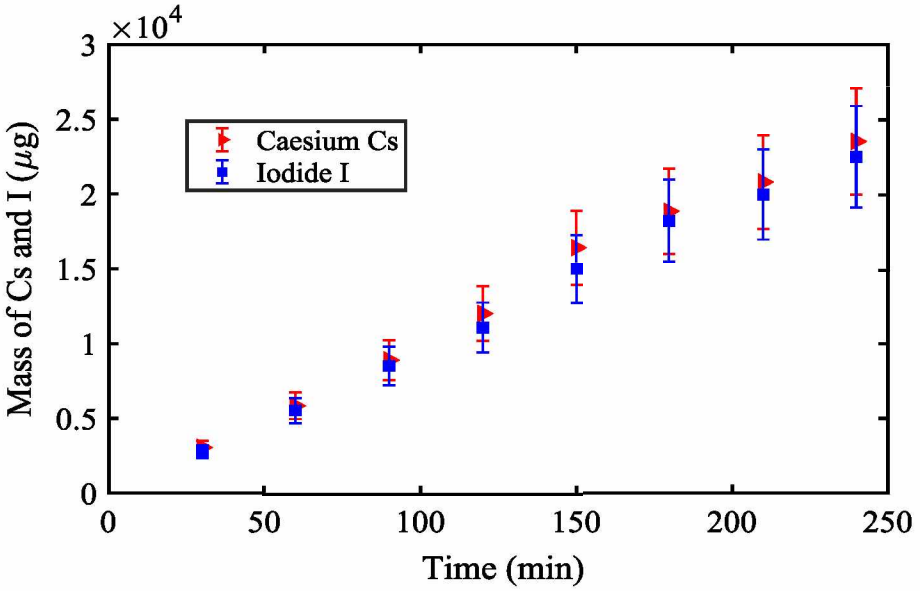

Figure 6- Quantity of caesium Cs and iodide I trapped in the pool for test 6.

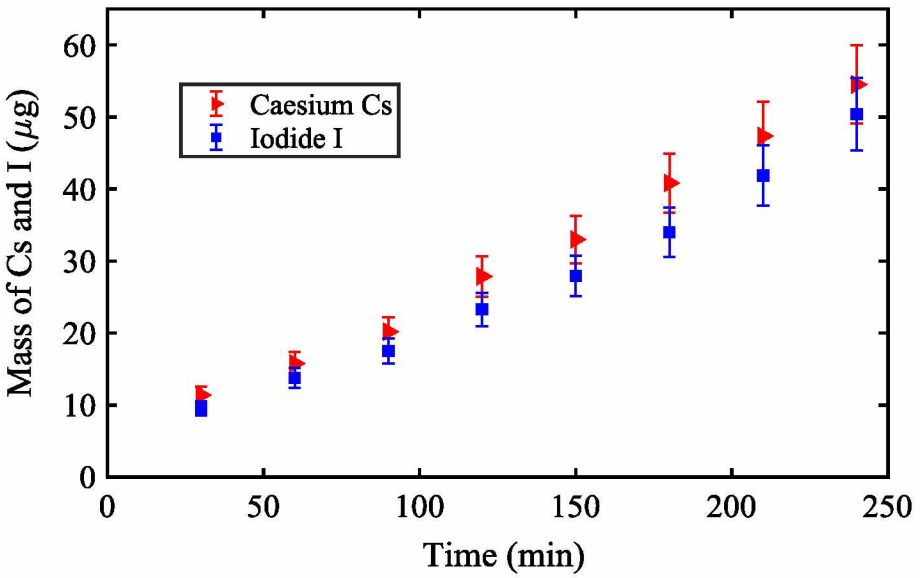

Figure 7- Mass of caesium Cs and iodide I collected in the bubblers of the sampling line for test 6 (Q_{inj} = 77.6 L/min and $Q_{sampling}$ = 3.5 L/min).

Figure 8 depicts the molar ratio of caesium to iodide trapped in the pool and the sampling system. This ratio shows that the trapped and released species remained in form of caesium iodide CsI and did not present decompositions into other mixtures.

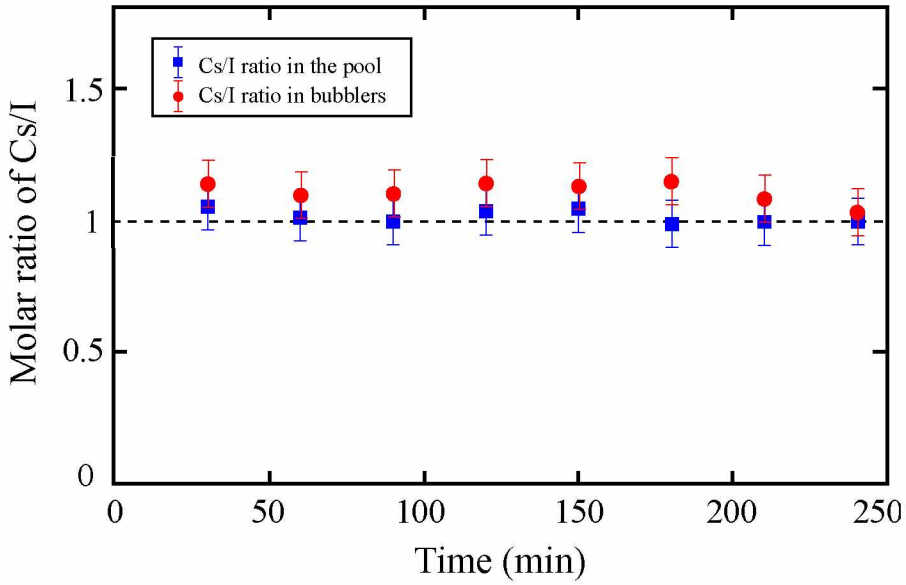

Figure 8- Molar ratio of caesium and iodide species trapped in the pool and sampling system.

On the other side, it is worth mentioning that the deposition of aerosols on the tubing was found to be important regardless of the test conditions. Table 4 presents the mass quantities of trapped CsI in the tubing, bubblers, and the deposition of aerosols on the filter after multiplying by the dilution factor shown in eq.(5). Therefore, this highlights that the washing of all the sampling line is very important for the determination of the decontamination factor, to collect all the possible depositions and consider them.

Table 4- Retention and deposition in the sampling line for Test 6.

Test	Deposition on the tubing	Retention in bubblers	Deposition on the terminal fiber filter
Test 6	676 µg	2287 µg	737 µg

3.2.2. Hydrodynamic aspects and dependence on flow regime

According to the transition criterion of Zhao et al. [36], we considered a transition regime between the bubby regime and jet regime as shown in Figure 9. The transition regime corresponds the range of a Weber number such that to $150 < We < 300$, as shown in Figure 10. In this range the flow morphology could not be described as bubbly because the large rate of coalesced bubbles introduces vertically elongated gas structures (no globule formation), on the other hand, there is no continuous gas jet.

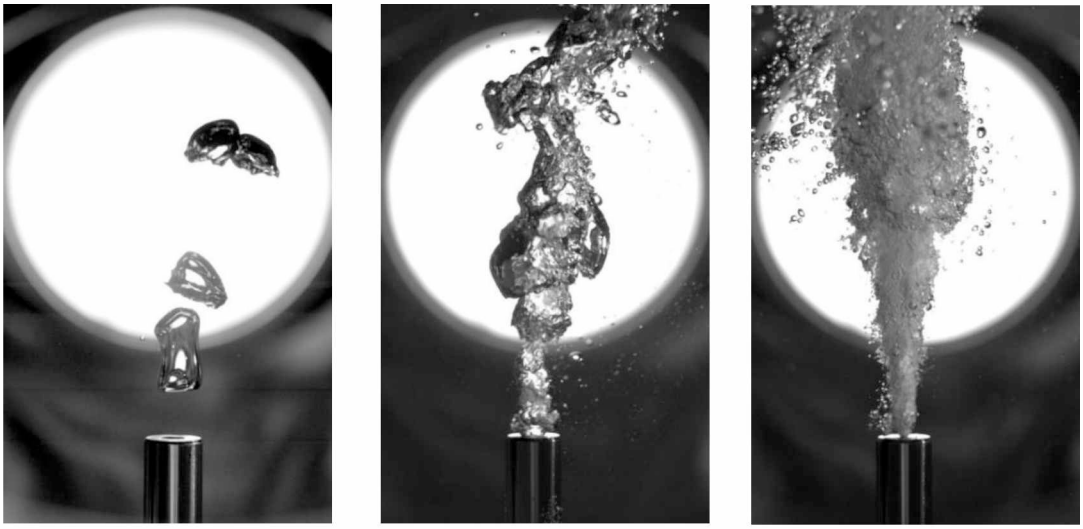

(a) (b) (c)

Figure 9- The morphology of flow for the different regimes; (a): We = 0.8 for bubbly regime, (b): We = 205 for transition regime, (c) We = 15600 for jetting regime.

(a) (b) (c)

Figure 10- Transition regime for 150 < We < 300; (a): D_0 = 2 mm, We = 205; (b): D_0 = 5 mm, We = 250; (c): D_0 = 10 mm, We = 260.

Figure 11 shows the variation of decontamination factor measurements as a function of the nozzle size as well as the injection flowrate, realized throughout our experiments. Regarding the nozzle size, the increasing of nozzle diameter D_0 from 2 mm to 5 mm hindered the scrubbing efficiency at high flowrates (Q_{inj} = 33 L/min, 75 L/min, 131 L/min), while the latter was favored for low flowrate Q_{inj} = 9 L/min. Inversely, increasing the nozzle size from 5 mm to 20 mm favored the scrubbing efficiency for the injection flowrate Q_{inj} = 75 L/min, and the same impact was reported for the low flowrate Q_{inj} = 9 L/min.

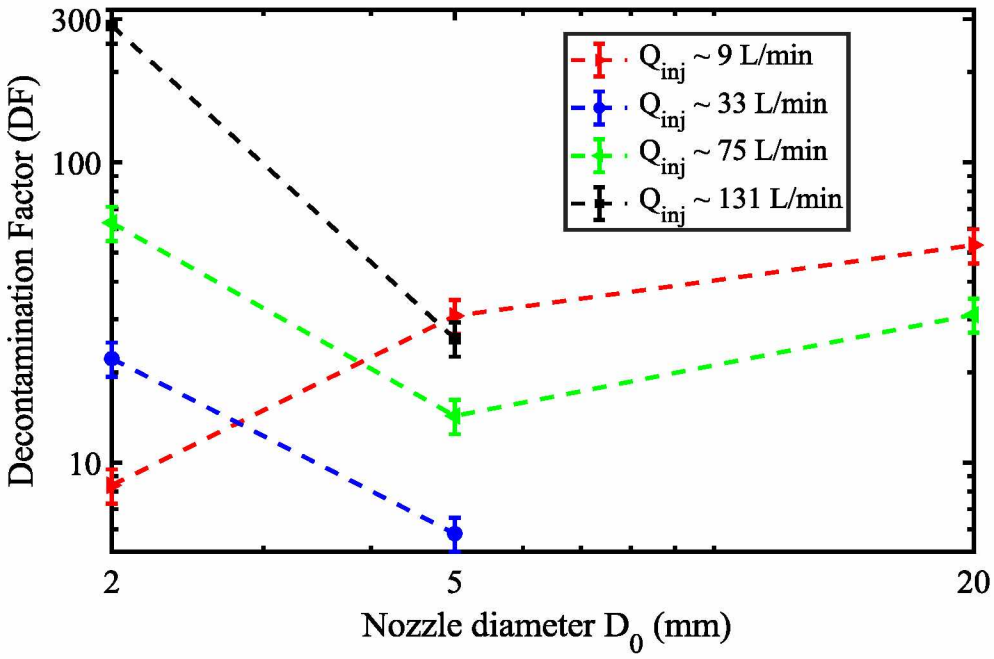

Figure 11- The effect of injection flowrate and nozzle size on the decontamination factor of CsI aerosols.

On the other hand, the higher was the injection flowrate the better was the scrubbing efficiency at nozzle D_0 = 2 mm. Then, at D_0 = 5 mm, the highest DF was reported for the lowest flowrate, and beyond that the scrubbing efficiency was favored for the higher flowrate. However, at D_0 = 20 mm, the scrubbing efficiency was greater for the lower flowrate.

Therefore, an important message can be concluded, which is that there is no unique sense of impact on the scrubbing efficiency from neither the nozzle size nor the injection flowrate. Indeed, through the literature review highlighted in the introduction (see 1), the injection flowrate has shown opposite senses between an experimental work and another. Herranz et al. [22] and Yoon et al. [24] reported a favorable impact due to the inertial impaction induced by the increase of injection flowrate. On the other side, unfavorable impact was observed by Xu et al. [25] and Beghi et al. [26], and a competitive effects was reported by Li et al. [27] and Woo et al. [23].

Taking into considerations these countereffects, an analytical approach is considered using the Weber number as it compares the inertial forces influenced by both the injection velocity and the nozzle size. Figure 12 presents the experimental decontamination factors as function of Weber number. The tests conditions of our experimental work and for the different works are similar. In other words, the temperature of the pool and gas were ambient, no steam in gas mixture, vertical single injector, and submergence of nozzle ranged between 90 and 100 cm. The variable parameters are the nozzle size and injection flowrate, eventually the Weber number.

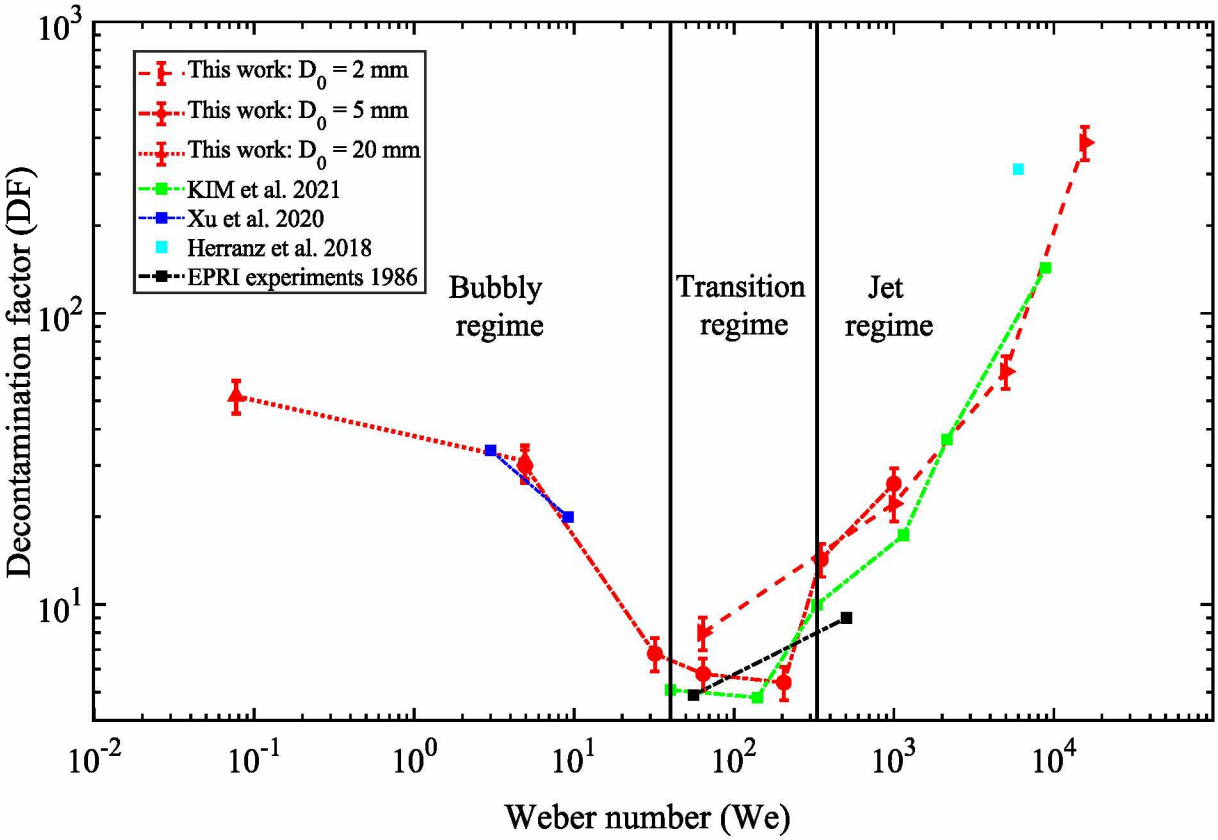

Figure 12- The variation of decontamination factor as function of injection flowrate and nozzle size in terms of Weber number, data from this work compared to literature data using different experimental conditions; Kim et al. [29] (Same gas flowrate for different nozzle diameters; D_0 = 5 mm, 8 mm, 10 mm, 15 mm, 20 mm, 30 mm), Xu et al. [25] (D_0 = 25 mm), Herranz et al. [22] (D_0 = 6.5 mm), and EPRI experiments [16] (D_0 = 12.7 mm).

Two major and important observations are shown in Figure 12, which can illustrate the discrepancy of the impact of injection flowrate Q_{inj} and nozzle size D_0 on the decontamination factor DF:

- Relevance of using the Weber number that comprise both D_0 and Q_{inj},
- Existence of a We corresponding to minimum scrubbing efficiency.

Characterization of DF with Weber number

The use of Weber number for pool scrubbing tests showed a good estimation of decontamination factor, despite the variation of nozzle size D_0 and injection flowrate Q_{inj} in Figure 12. To recall, the Weber number is a criterion for the classification of flow regimes, which indicates that the DFs are varying according to the flow regime. Therefore, one cannot analyze the effect of Q_{inj} without taking consideration of D_0 and vice versa, because one parameter of these parameters is sufficient to shift from a flow regime to another. This justifies why no clear impact could be concluded from neither D_0 nor Q_{inj} in Figure 11.

Moreover, the different trends of the decontamination factor observed in Figure 12 consolidate and clarify the finding of Herranz et al. [22], Yoon et al. [24], Xu et al. [25], Beghi et al. [26], Li et al. [27], and Kim et al. [29]. These experimental works reported different impacts of

injection flowrate or nozzle size, because the examination was performed in different flow regimes and analyzed according, and here the importance of characterization the flow by the Weber number is revealed.

Existence of minimum scrubbing efficiency

The notion of minimum scrubbing efficiency stems from the countereffects of aerosol removal mechanisms for the different experimental configurations. Swiderska et al. [16] reported that an increase in gas flowrate favors the inertial and centrifugal impaction, but it hinders the residence time. Through the analysis of Figure 12 given below, this is clearer according to the different flow regimes.

At low Weber number ($0.08 < We < 10$), where flow regime is described as bubbly regime with formation of globules and bubbles, the obtained DFs are relatively high but follow a decreasing trend. In this regime, a main factor influences DF: the residence time of the injected gas in the pool. The residence time, which is correlated to gas injection velocity Q_{inj} [16, 33],will increase with the decrease of Weber number (injection flowrate lower or nozzle size larger). Hence, as this parameter is greater, the aerosol removal mechanisms will act for longer period of time promote trapping efficiency. This can be shown in the modelling of the latter aerosol removal mechanisms (i.e., sedimentation, centrifugal impaction, and diffusion) reported by Swiderska et al. [16].

Beyond this, as the Weber number increases introducing the transition phase referred as churn turbulent regime, the DF exhibits a sharp decrease. A minimum of DF for the different experimental works, including our work, is reported in this range of Weber number corresponding to this flow regime ($150 < We < 300$). At this regime, same aerosol removal mechanisms will act as in the previous regime, however, for less residence time.

Beyond that, and as Weber number indicates the onset of jetting regime ($We \approx 330$), the DF increases as the Weber increases ($We > 300$). Although that residence time is not important anymore, but as inertia dominates in this regime, aerosols are trapped by regime-induced removal mechanism, namely inertial impaction. This is due to the fact that aerosols possess momentum that can deviate them from streamlines. This mechanism, inertial impaction, is represented by the dimensionless Stokes number, corresponding to the ratio of the stopping distance S of a particle to a characteristic dimension of the problem [40], here the nozzle diameter D_0:

$$St = \frac{S}{D_0} = \frac{\tau_p U_{inj}}{D_0} \tag{6}$$

where τ_p is the relaxation time of the particle, U_{inj} is the gas injection velocity and D_0 is the nozzle diameter. In the range of particle sizes and flowrates considered in our study, maximum values of particle Reynolds number $Re_p = \frac{\rho_g d_p U_{inj}}{\mu_g}$ remain close to 1 (Stokes regime), thus τ_p can be expressed as [40]:

$$\tau_p = \frac{\rho_p \ {d_p}^2 C_c}{18\,\mu_g} \tag{7}$$

where ρ_p is the aerosol density, d_p is the particle aerodynamic diameter, μ_g is the dynamic viscosity of gas and C_c the Cunningham slip correction factor. This latter being close to 1 for aerodynamic diameter greater than 0.1 µm [40], Stokes number can be written as:

$$St = \frac{\rho_p \ {d_p}^2 U_{inj}}{18 \, \mu_g \, D_0} \tag{8}$$

The decontamination factor by the inertial impaction mechanism is determined by:

$$DF_{imp} = \frac{1}{1 - Eff} \tag{9}$$

Where Eff_{imp} is the efficiency of deposition due to the jet impaction, knowing that Eff_{imp} can be expressed as a function of *St*. Indeed, through literature, different correlations are proposed to describe the efficiency deposition [42, 43]. Through our approach of estimating the retention of aerosols by inertial impaction, the correlation developed in literature by He al. [43] is considered.

$$Eff_{imp} = \begin{cases} 1.79182 \ (3.4337 \times 10^{-11})^{(5.9244 \times 10^{-3})^{\sqrt{St}}} & \sqrt{St} \leq 0.65868 \\ 1.13893 \ (1.4173 \times 10^{-6})^{(4.25973 \times 10^{-3})^{\sqrt{St}}} & \sqrt{St} > 0.65868 \end{cases} \tag{10}$$

Through the determination of decontamination factor due to inertial impaction in eq.(9) and eq.(10), it is revealed that a major trapping in the jetting regime occurs due to the mechanism of inertial impaction in the range around $0.7 < St < 2$ (corresponding approximately to $1000 < We \ 5000$), as shown in Figure 13. Indeed, in this range, experimental values are close to the model curve considering only aerosol impaction.

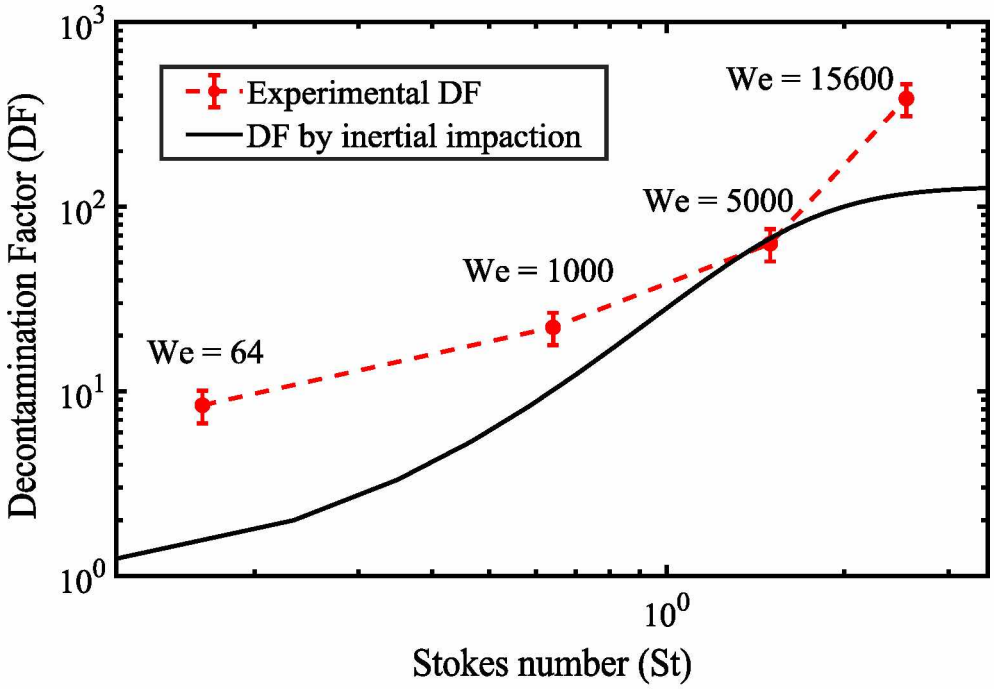

Figure 13- Comparison between experimental DF and the calculated DF determined by inertial impaction for tests 1 (We = 64), 2 (We = 1000), 3 (We = 5000), and 4 (We = 15600).

Moreover, as Weber number increases in jetting regime (We > 5000, St > 2), another mechanism might contribute to the retention of aerosols since experimental values are higher than impaction model. This is very probably due to a higher interfacial area between the gas and liquid phase that occurs, thus enhancing the transfer between these two phases. The flow breaks rapidly into tiny bubbles due to high inertial and turbulent flow [24], at a closer distance from the nozzle, as shown in Figure 9-(c). The higher the Weber, the higher is the inertia of flow; therefore, the more the breakup is rapid leading to tiny bubbles distribution in the pool [44].

Kim et al. [29] carried out experimental work to analyze the effect of the nozzle size. For same injection flowrate, experiments were carried out using five sizes of nozzles, where they reported an increase of scrubbing efficiency when the nozzle diameter decreases. In fact, as nozzle size decreases, Weber number increases. Since the flow regimes examined by Kim et al. [29] were jetting as shown in Figure 12, therefore, the further decrease in the nozzle size for the same flowrate will increase the Stokes number, thus increasing the inertial impaction as well as the interfacial area between the bubbles and the pool. However, this finding would not be consistent if one examined the impact of nozzle size in bubbly regimes since the decrease of nozzle size in this case will hinder the decontamination factor due to the decrease of residence time and absence on inertial impaction.

3.2.3. Dependence on the pool submergence

Pool submergence is an important test parameter favoring the retention of aerosols. However, its sensitivity depends significantly on the different control variables of pool scrubbing experiments. Figure 14 and Figure 15 presents decontamination factors at different submergences for bubbling and jetting regimes respectively.

Submergence in case of bubbling regime

In case of bubbly regime (see Figure 14), the nozzle size D_0 = 2 cm was used, gas and pool temperature were adjusted at 25 °C, injection flowrate was regulated at 9.21 L/min and pool pH was set to 7. The other test conditions are shown in Table 5.

Table 5- Summary of tests examining the impact of pool submergence

Test	Weber	Pool level (cm)	Volume of liquid in the column (m^3)	Average Residence time $\tau_{average}$ (s)	DF (± 10%)
12	0.08	100	0.1964	2.1	46
13	0.08	30	0.0589	0.62	18
14	0.08	10	0.0196	0.21	6

In this study, the average residence time of bubbles can be approximated as presented in eq (11).

$$\tau_{average} = {H_{pool}}/{U_{injection}} \qquad (11)$$

In this approximation, it is not intended to calculate the actual residence time, but to give the difference in order of magnitude when varying the level of liquid in the pool as shown in Table 5.

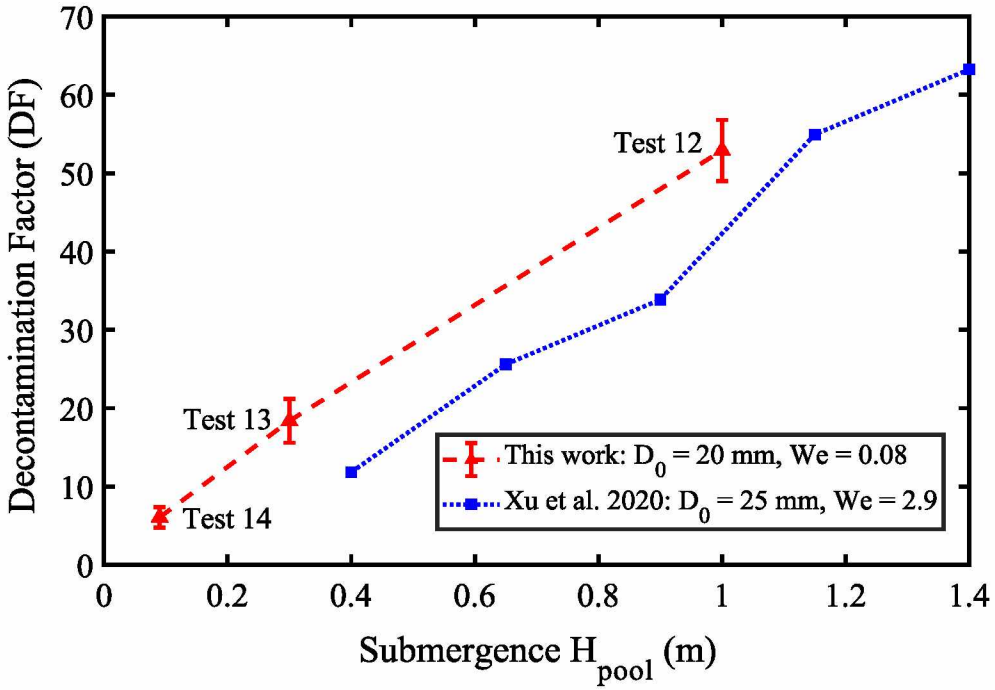

Figure 14- The impact of submergence on DF in bubbly regimes at We = 0.08 with comparison at We = 2.9 from Xu et al. [25].

Various factors promote the retention of CsI aerosols as the submergence increases: increase of residence time τ, hygroscopic growth of soluble CsI aerosols size and development/exhibition of a steady state of bubbles swarm at a sufficient submergence.

Regarding the hygroscopic growth, the size of aerosols particles increases as the relative humidity of carrier gas increases when it rises in the pool, as reported by Li et al. [27]. The evolution of aerosol size makes larger particles easier to retain than small ones, due to the mechanism of deposition [16, 27, 31]. It is suggested that this effect occurred in our experiments, when the pool submergence increased from 10 cm to 100 cm.

Despite the attenuation of retention due to decrease in the submergence, test 14 that represents the altitude of injection zone, shows that the contribution of this zone in aerosol retention is also important (DF = 6.1). This agrees with the analysis performed by Lee et al. [45] to reveal the contribution of the injection zone to the scrubbing of aerosols.

Submergence in case of jetting regime

In case of jetting regime (see Figure 15), the decontamination factor measurements carried out at H_{pool} = 100 cm converge with the experiments realized by Yoon et al. [24] with relatively same Weber number but at H_{pool} = 50 cm. The scrubbing efficiency shows no difference between the two configurations despite the change of pool submergence between 50 cm and 100 cm. It can be noted that for low pool submergence, such that H_{pool} < 100 cm, the level of pool could not be sufficient for the exhibition of the third hydrodynamic zone, i.e., the bubble rise zone. Therefore, it is suggested that the main major mechanism responsible for the aerosols' removal will be the inertial impaction that occurs near the nozzle as shown in Figure 13.

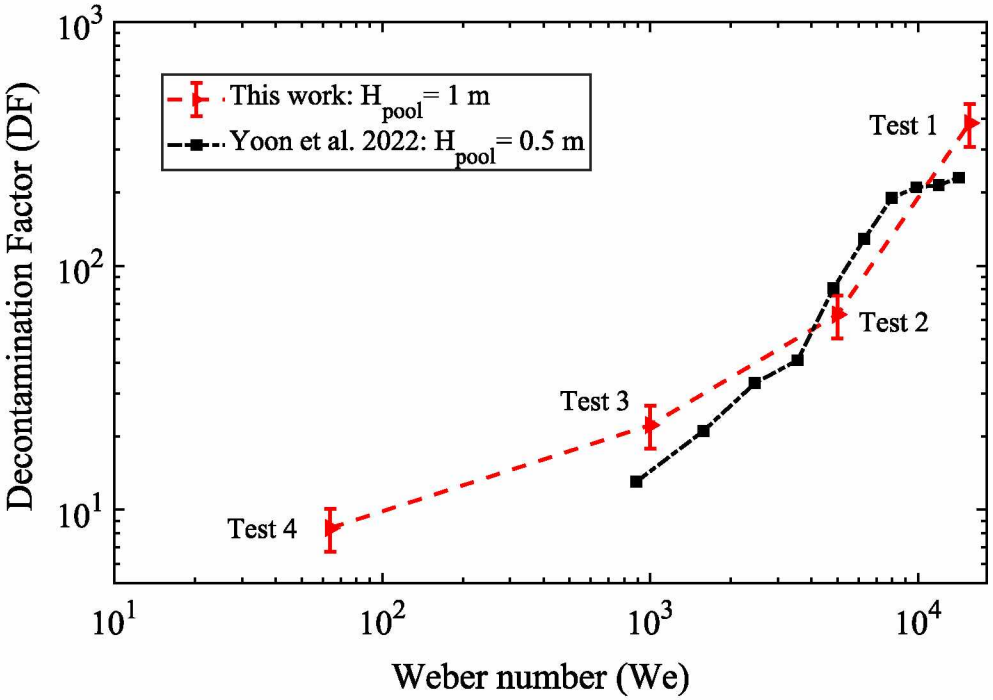

Figure 15- The influence of submergence in case of jetting regime; and Yoon et al. [24].

This suggestion is consolidated by Herranz et al. [44], as they considered that inertial impaction is the dominant removal mechanism in jetting regimes for pool submergences $H_{pool} \leq 1.25$ m, and when the orifice is vertically oriented. On the other hand, the slope variation for Yoon et al. [24] beyond We = 10^4 as their DF tends to asymptotic limitation shows the asymptotic behavior of inertial impaction discussed on Figure 13, especially when taking in consideration their low pool submergence. Whereas, in our experiments where pool submergence is higher, the increase in interfacial area contributes beyond the boundaries of inertial impaction as shown in Figure 13.

4. Conclusion

Pool scrubbing is a mean of filtration that aims at reducing the release of fission products following a nuclear accident. Experimental campaign of decontamination factor measurements has been performed to study mainly hydrodynamic aspects of aerosols trapping by pool scrubbing. The potential influences of injection flowrate and nozzle size were investigated and characterized in terms of Weber number.

According to the realized experimental work, the following conclusion can be drawn:

- The pool scrubbing efficiency is significant due to the dependence of aerosol removal mechanisms on the hydrodynamic aspects. The countereffects of gas flowrate and nozzle size were characterized by a Weber number, which is used to classify the flow regimes. This approach seems to be efficient and consistent in dimensionless analysis of the decontamination factor, when compared to different experimental works.

- The impact of injection flowrate Q_{inj} and nozzle size D_0 can induce countereffects, favoring and hindering the retention of aerosols by pool scrubbing. However, the sense of their impact depends on the examined flow regime. As the change of these two parameters tends the flow toward the transition regime, then, this would lead to unfavorable impact and vice versa.

- A minimum of decontamination factor presents in the transition zone between bubbly and jetting regime, due to the week sensitivity of aerosol removal mechanisms in this zone, mainly to low residence time and absence of inertial impaction.

- Throughout our examination, we shown the important influence of residence time in bubbly regime, that led to high scrubbing efficiency.

- On the other hand, the inertial impaction at the jetting regime and increase of interfacial area led to high and increasing scrubbing efficiency, when the Weber number indicates a flow regime beyond the transition zone.

- The pool submergence has been more important in bubbly regime than in case of jetting regime. This due to the fact, larger submergence induces higher residence, whereas in jetting regime, inertial impaction is the dominant mechanism as the height of pool does not permit the generation and expansion of bubbles swarm with tiny bubbles.

Acknowledgement

This work was performed in the French Institut de Radioprotection et de Sûreté Nucléaire (IRSN), with the financial support of French Région Sud - Provence-Alpes-Côte d'Azur and Electricité de France (EDF).

References

1. Jacquemain, D., S. Guentay, S. Basu, M. Sonnenkalb, L. Lebel, J. Ball, H. J. Allelein et al. *OECD/NEA/CSNI status report on filtered containment venting*. No. NEA-CSNI-R--2014-7. Organisation for Economic Co-Operation and Development, 2014.

2. Beahm, E. C., C. F. Weber, T. S. Kress, and G. W. Parker. *Iodine chemical forms in LWR severe accidents. Final report*. No. NUREG/CR-5732; ORNL/TM-11861. Nuclear Regulatory Commission, Washington, DC (United States). Div. of Systems Research; Oak Ridge National Lab., TN (United States), 1992.

3. Nuclear Regulatory Commission. *Technical bases for estimating fission product behavior during LWR accidents. Technical report*. No. NUREG--0772. Nuclear Regulatory Commission, 1981.

4. Shahbazi, Shayan, Sara Thomas, Dong Hoon Kam, and David Grabaskas. "State of Knowledge on Aerosols and Bubble Transport for Mechanistic Source Term Analysis of Molten Salt Reactors.", 2022.

5. Jacquemain, D., S. Guentay, S. Basu, L. Lebel, H-J. Allelein, B. Liebana, B. Eckardt, L. Ammirabile, and T. Nitheanandan. *Summary of OECD/NEA status report on filtered containment venting*. No. AECL-CW--126500-CONF-004. Atomic Energy of Canada Limited, 2015.

6. Gupta, Sanjeev, Benjamin Balewski, Karsten Fischer, and Gerhard Poss. "Experimental investigations of BWR pressure suppression pool behaviour under loss of coolant accident conditions." *ICAPP-11, Paper* 11389 (2011).

7. Welker, Marina. "AREVA's containment venting technologies and experience worldwide." In *41st Annual Meeting of the Spanish Nuclear Society*. 2015.

8. Ramsdale, S. A., G. J. Bamford, S. Fishwick, and H. C. Starkie. "Status of research and modelling of water-pool scrubbing." (1992).

9. Cunnane, J. C., M. R. Kuhlman, and R. N. Oehlberg. *Scrubbing of fission product aerosols in LWR water pools under severe accident conditions-experimental results*. No. EPRI-NP--4113-SR. 1985.

10. McCormack, J. D., D. R. Dickinson, and R. T. Allemann. "Experimental results of ACE vent filtration." *Pool Scrubber Tests AA1-AA4 and DOP1-DOP5 (No. ACETR-A1)* (1989).

11. Marcos, M. J., F. J. Gómez, I. Melches, M. Martín, and M. Lopez. "Lace-Espana experimental programme on the retention of aerosols in water pools." (1994).

12. Hashimoto, K. "High pressure pool scrubbing experiment for a PWR severe accident." *Proc. Int. Top. Mtg. Safety of Thermal Reactors, Portland, July, 1991* (1991).

13. Hashimoto, K., K. Soda, S. Uno, H. Nakatani, and H. Tateoka. "Effect of pool scrubbing of insoluble aerosol in two phase flow in a pipe." In *Severe accidents in nuclear power plants*, 1988.

14. Hillary, J., J. C. Taylor, F. Abbey, and H. R. Diffey. "Iodine removal by a scale model of the SGHW reactor vented steam suppression system." *No. TRG Report* 1256, 1966.

15. Güntay, S. "Experiment poseidon: Elemental iodine retention in water pools." *Transactions of the American Nuclear Society;(USA)* 62, no. CONF-901101, 1990.

16. Swiderska-Kowalczyk, M., M. Escudero-Berzal, M. Marcos-Crespo, M. Martin-Espigares, and J. Lopez-Jimenez. "State-of-the-art review on fission product aerosol pool scrubbing under severe accident conditions, 1996.

17. Steinhauser, George, Alexander Brandl, and Thomas E. Johnson. "Comparison of the Chernobyl and Fukushima nuclear accidents: a review of the environmental impacts." *Science of the total environment* 470, 2014.

18. National Research Council. *Lessons learned from the Fukushima nuclear accident for improving safety of US nuclear plants*, 2014.

19. Jacquemain, D., T. Albiol, S. Dickinson, L-E. Herranz, F. Funke, G. Glowa, S. Gupta et al. "Conclusion of the International OECD/NEA-NUGENIA Iodine Workshop." In *11th International Topical Meeting on Nuclear Reactor Thermal Hydraulics, Operation and Safety, NUTHOS-11*, 2016.

20. Jacquemain, Didier, Gerard Cenerino, Francois Corenwinder, Emmanuel IRSN Raimond, Ahmed Bentaib, Herve Bonneville, Bernard Clement et al. "Nuclear power reactor core melt accidents. Current State of Knowledge, 2015.

21. Albiol, T., L. Herranz, E. Riera, C. Dalibart, T. Lind, A. Del Corno, Teemu Kärkelä et al. "Main results of the European PASSAM project on severe accident source term mitigation." *Annals of Nuclear Energy* (116), 2018.

22. Herranz, Luis E., Claudia Lopez, and Jaime Penalva. "Investigation on jet scrubbing in nuclear reactor accidents: From experimental data to an empirical correlation." *Progress in Nuclear Energy* 107 (2018): 72-82.

23. Jung, Woo Young, Dong Young Lee, Ji-Hoon Kang, Min-Seok Ko, Beom Kyu Kim, Jongchan Lee, Doo Yong Lee, Byeonghee Lee, and Kwang Soon Ha. "Experimental study of pool scrubbing under horizontal gas injection." *Annals of Nuclear Energy* 171, 2022.

24. Yoon, Jongwoong, Yo Han Kim, and Yong Hoon Jeong. "Observation of the jet transition at a single vertical nozzle under pool scrubbing conditions." *Annals of Nuclear Energy* 171, 2022.

25. Xu, Youyou, Jian Deng, Zhiqiang Zou, Guangming Jiang, and Xiaoli Wu. "Experimental study on aerosol behavior in water pool scrubbing under severe accident

conditions." *International Journal of Advanced Nuclear Reactor Design and Technology* 2, 2020.

26. Beghi, Ignazio, Terttaliisa Lind, and Horst-Michael Prasser. "Experimental studies on retention of iodine in a wet scrubber." *Nuclear Engineering and Design* 326, 2018.

27. Li, Yingzhi, Zhongning Sun, Haifeng Gu, and Yanmin Zhou. "Deposition characteristic of micro-nano soluble aerosol under bubble scrubbing condition." *Annals of Nuclear Energy* 133, 2019.

28. Li, Yuxiang, Lili Tong, and Xuewu Cao. "Experimental study on influencing factors of aerosol retention by pool scrubbing." *Frontiers in Energy Research* 9, 2021.

29. Kim, Yo Han, Jongwoong Yoon, and Yong Hoon Jeong. "Experimental study of the nozzle size effect on aerosol removal by pool scrubbing." *Nuclear Engineering and Design* 385, 2021.

30. Vennemann, René, Michael Klauck, and H-J. Allelein. "Experimental Investigation on the Retention of Soluble Particles by Pool Scrubbing." *Journal of Nuclear Engineering and Radiation Science* 8, no. 4, 2022.

31. Dehbi, A., D. Suckow, and S. Guentay. "Aerosol retention in low-subcooling pools under realistic accident conditions." *Nuclear engineering and design* 203, no. 2-3, 2001.

32. Berna, C., A. Escrivá, J. L. Muñoz-Cobo, and Luis E. Herranz. "Enhancement of the SPARC90 code to pool scrubbing events under jet injection regime." *Nuclear Engineering and Design* 300 (2016): 563-577.

33. Owczarski, P. C., and K. W. Burk. *SPARC-90: A code for calculating fission product capture in suppression pools*. No. NUREG/CR-5765; PNL-7723. Nuclear Regulatory Commission, Washington, DC (United States). Div. of Regulatory Applications; Pacific Northwest Lab., Richland, WA (United States), 1991

34. Farhat, M., Chinaud, M., Nerisson, P., Vauquelin, O. "Characterization of bubbles dynamics in aperiodic formation." *International Journal of Heat and Mass Transfer* 180 (2021): 121646.

35. Gaddis, E. S., and A. J. C. E. S. Vogelpohl. "Bubble formation in quiescent liquids under constant flow conditions." *Chemical Engineering Science* 41, no. 1 (1986): 97-105.

36. Zhao, Y-F., and Gordon A. Irons. "The breakup of bubbles into jets during submerged gas injection." *Metallurgical Transactions B* 21, no. 6, 1990.

37. Kyriakides, N.K., et al., *Bubbling from nozzles submerged in water: Transitions between bubbling regimes.* The Canadian Journal of Chemical Engineering, 1997. **75**(4): p. 684-691.

38. Cai, Qingbai, Xuesong Shen, Chunyin Shen, and Gance Dai. "A simple method for identifying bubbling/jetting regimes transition from large submerged orifices using

electrical capacitance tomography (ECT)." *The Canadian Journal of Chemical Engineering* 88, no. 3, 2010.

39. Bosland, L, Leroy, O., Alvarez, C. Chebbi, M. Monsanglant-Louvet, C. Bourrous, S., Chevalier-Jabet, K. "Study of the stability of CsI and iodine oxides (IOx) aerosols and trapping efficiency of small aerosols on sand bed and metallic filters under irradiation." *Progress in Nuclear Energy* 142 (2021): 104013.

40. Hinds, William C., and Yifang Zhu. *Aerosol technology: properties, behavior, and measurement of airborne particles*. John Wiley & Sons, 2022.

41. Davidson, Leon, and Erwin H. Amick Jr. "Formation of gas bubbles at horizontal orifices." *AIChE Journal* 2, no. 3, 1956.

42. Clift, Roland, John R. Grace, and Martin E. Weber. "Bubbles, drops, and particles.", 2005.

43. Herranz, L. E., A. Cabrer, and V. Peyres. "Modelling inertial impaction within pool scrubbing codes." *Journal of aerosol science* 31, 2000.

44. He, L. W., Y. X. Li, Y. Zhou, S. Chen, L. L. Tong, and X. W. Cao. "Investigation on aerosol pool scrubbing model during severe accidents." *Frontiers in Energy Research*, 2021.

44. Herranz, Luis E., Virginia Peyrés, Jesús Polo, María J. Escudero, Manuel M. Espigares, and José López-Jiménez. "Experimental and analytical study on pool scrubbing under jet injection regime." *Nuclear technology* 120, no. 2, 1997.

45. Lee, Yoonhee, Yong Jin Cho, and Inchul Ryu. "Preliminary analyses on decontamination factors during pool scrubbing with bubble size distributions obtained from EPRI experiments." *Nuclear Engineering and Technology* 53, no. 2, 2021.